Technological University Dublin
ARROW@TU Dublin

Articles | Photonics Research Centre

2019

Third-order optical nonlinearity properties of CdCl2-modifed Ge–Sb–S chalcogenide glasses

Xiaosong Lu

Jianhui Li

Lu Yang

See next page for additional authors

Follow this and additional works at: https://arrow.tudublin.ie/prcart

 Part of the Electrical and Computer Engineering Commons, and the Optics Commons

This Article is brought to you for free and open access by the Photonics Research Centre at ARROW@TU Dublin. It has been accepted for inclusion in Articles by an authorized administrator of ARROW@TU Dublin. For more information, please contact arrow.admin@tudublin.ie, aisling.coyne@tudublin.ie, gerard.connolly@tudublin.ie.

This work is licensed under a Creative Commons Attribution-Noncommercial-Share Alike 4.0 License
Funder: National Natural Science Foundation of China; Natural Science Foundation of Heilongjiang Province of China; Romanian Ministry of Research and Innovation;

Authors

Xiaosong Lu, Jianhui Li, Lu Yang, Runan Zhang, Yindong Zhang, Jing Ren, Aurelian Catalin Galca, Mihail Secu, Gerald Farrell, and Pengfei Wang

Journal of Non-Crystalline Solids 528 (2020) 119757

Contents lists available at ScienceDirect

Journal of Non-Crystalline Solids

journal homepage: www.elsevier.com/locate/jnoncrysol

Third-order optical nonlinearity properties of $CdCl_2$-modifed Ge–Sb–S chalcogenide glasses

Xiaosong Lu[a], Jianhui Li[a], Lu Yang[a], Runan Zhang[a], Yindong Zhang[a], Jing Ren[a,*], Aurelian Catalin Galca[b], Mihail Secu[b], Gerald Farrell[c], Pengfei Wang[a,d,*]

[a] Key Lab of In-fiber Integrated Optics, Ministry Education of China, Harbin Engineering University, Harbin 150001, China
[b] National Institute of Materials Physics, Laboratory of Multifunctional Materials and Structures, 105bis Atomistilor Street, PO Box MG—36, RO-77125, Magurele, Romania
[c] Photonics Research Centre, Technological University Dublin, Kevin Street, Dublin 8, Ireland
[d] Key Laboratory of Optoelectronic Devices and Systems of Ministry of Education and Guangdong Province, College of Optoelectronic Engineering, Shenzhen University, Shenzhen, 518060, China

ARTICLE INFO

Keywords:
Chalcohalide glasses
Third-order optical nonlinearity
Two-photon absorption
Z-scan technique

ABSTRACT

We developed a new type of chalcohalide glasses with physicochemical and nonlinear optical properties that are tunable by composition. It is found that more than 60 mol.% $CdCl_2$ heavy metal halide can be dissolved into the ternary Ge–Sb–S system and forming stable glasses. The visible-light transparency range is extended to shorter wavelengths with the addition of $CdCl_2$, which is beneficial for the optical quality control and infra-red (IR) system alignment. The third-order optical nonlinearity (TONL) is studied using the femtosecond Z-scan method. The results show that both the nonlinear refractive index and two photon absorption co-efficient decrease with $CdCl_2$. Benefiting from the favorable property-tailoring effects of $CdCl_2$, the TONL figure of merit (FOM) can be improved to meet the requirement (FOM $<$ 1) for all-optical switching and IR photonic applications.

1. Introduction

Chalcogenide glasses (ChGs), due to their broadband infra-red (IR) transparency, outstanding third-order optical nonlinearity (TONL) and ease of processing and integration, have attracted worldwide interest for integrated IR photonics [1,2] and all-optical-signal processing [3,4]. Particularly, arsenic-free ChG glasses based on the ternary Ge–Sb–S system have been proven to be instrumental to diverse applications because of: 1) the broad glass forming region which entails convenient tuning of composition-dependent properties (e.g., refractive index, bandgap), 2) waveguiding capacity for light confinement which is essential for gas sensing [5], and 3) remarkably large nonlinearities (two orders of magnitude of SiO_2) which make super-continuum generation possible in a broad IR region (1–5 μm) [6,7].

In the Ge–Sb–S system, the nonlinear refractive index (n_2) of glass increases with the Sb_2S_3 content. However, the glass with a large Sb_2S_3 concentration becomes opaque in the visible-light region as a result of the shrinkage of optical bandgap [8]. Such a problem renders the optical quality control and IR system alignment very complicated. Benefiting from an extended visible-light transparency range and limited two-phonon absorption (TPA), metal-halide (e.g., CsCl) modified ChGs, also known as chalcohalide glasses, are becoming promising IR photonic materials for nonlinear optical applications [9–13].

In this paper, we proposed a novel chalcohalide glass system. It is surprisingly found that more than 60% $CdCl_2$ heavy metal halide can be dissolved in the Ge–Sb–S system, which means that not only the physicochemical properties including the glass transition temperature, optical bandgap, linear refractive index etc. can be tailored, but also the nonlinearities such as the nonlinear refractive index, and TPA coefficient. As a consequence, an improved third-order nonlinear figure of merit (FOM) was achieved with FOM <1 as studied by the femtosecond Z-scan method. The newly developed chalcohalide glasses would be a promising material for waveguide parametric amplification and all-optical switching device.

2. Experiments

The (100-x) ($60GeS_2$-$40Sb_2S_3$, GeSbS in short). x $CdCl_2$ (x = 0, 10, 20, 30, 40, 50, 60, in mol.%) glass samples were prepared using the typical melt-quenching method. High purity Ge, Sb, S, $CdCl_2$ (5 N) were weighed in glove box purged with nitrogen gas, and then melted at 850 °C for 12 h in an evacuated (10^{-3} Pa) silica glass ampoule. The melts

* Corresponding authors at: Key Lab of In-fiber Integrated Optics, Ministry Education of China, Harbin Engineering University, Harbin 150001, China.
E-mail addresses: ren.jing@hrbeu.edu.cn (J. Ren), pengfei.wang@tudublin.ie (P. Wang).

https://doi.org/10.1016/j.jnoncrysol.2019.119757
Received 26 August 2019; Received in revised form 22 October 2019; Accepted 27 October 2019
Available online 04 November 2019
0022-3093/ © 2019 Elsevier B.V. All rights reserved.

were quenched at ambient temperature and then annealed at 200 °C for 5 h under vacuum.

X-ray diffractometer (XRD, D/MAX 2550VB/PC, Rigaku Corporation, Japan) was used with the Cu-Kα irradiation. The density was measured in alcohol (host liquid) via the Archimedes method. The glass transition temperatures were determined at a heating rate of 10 °C/min, in the atmosphere of flowing N_2 gas, using the differential scanning calorimeter (TA D2000, New Castle, DE). Optical transmission spectra were characterized by a Perkin-Elmer Lambda 950 UV–VIS spectrophotometer (500–2500 nm) and Bruker Tensor 27 Fourier transform infrared spectrophotometer (Ettlingen, Germany) (2.5–15 μm). Raman spectra were characterized by the Raman spectrometer (Renishaw inVia, Gloucestershire, UK, 532 nm excited).

The refractive index in the range of 500–1700 nm was measured by VASE (Variable Angle Spectroscopic Ellipsometry) J.A. Woollam Co., Inc. ellipsometry with rotating analyzer and angles of incidence 60°, 65° and 70°, respectively. A Cauchy model was used for the fitting. The back side of the samples was roughened before ellipsometry measurements to avoid the multiple reflections and to allow for the Psi and Delta data to be collected only from the front surface of glass. Attention was preferentially given to the linear refractive indices n_0 at 800 nm because the 800 nm femtosecond Ti: sapphire laser was used in Z-scan experiments. The TONL properties of glass samples were studied by the Z-scan technique using a Ti: sapphire laser (Mira 900-D, Coherent, USA), and more detailed parameters please refer to the reference [14]. Considering the inhomogeneity of samples, the Z-scan measurements were done on five different surface points for each sample, and only the averaged values were reported here [9].

3. Results and discussion

Optical transmission spectra and compositional variation of optical band gaps (E_g) of the samples are shown in Fig. 1(a) and (b), respectively. The transmittance of the samples is all above 65–70%, and the transparent window spans a range of 0.6 − 11 μm. The small bumps observed on the spectra are due to the absorptions related to the impurities such as –S-H-, OH- etc. [15]. When GeSbS is gradually substituted by $CdCl_2$, the short cut-off wavelength (λ_s, defined at the wavelength where the absorption coefficient is 10 cm^{-1}) presents a blue shift towards short wavelength, viz., from 627 nm ($x = 0$) to 572 ($x = 60$) nm, as shown in the locally magnified transmission spectra (inset of Fig. 1(a)). The blue shift of λ_s is caused by the E_g widening with the addition of $CdCl_2$, which can be interpreted by the empirical relationship [16]:

$$E_g = \frac{hc}{\lambda_s} \propto (\chi + \omega - \psi). \quad (1)$$

where h, c, χ, ω, ψ are respectively the Planck's constant, the velocity of light in vacuum, average electron affinity of anions, chemical bond energy, and polarization energy of anions. Cl has bigger electron affinity than S, viz., $\chi_{Cl} > \chi_S$. The polarizabilities of the elements follow such an order: Ge < Cd < Sb, and Cl < S [17]. The chemical bond energy is dependent on the electronegativity difference of the bonded atoms, which is manifested by the order $\omega_{Cl\text{-}Cd} > \omega_{Ge\text{-}S} > \omega_{Sb\text{-}S}$. Overall, with the substitution of GeSbS by $CdCl_2$, the value of ($\chi + \omega - \psi$) increases, which may account for the increasing E_g, and the blue-shift in λ_s. Besides, from the energy band structure point of view, the valence band top of ChGs is occupied by the lone pair electrons. It has been demonstrated that, by attracting and localizing the lone pair electrons, Cl atom can lower the nonbonding lone-pair electron levels, and thus enlarging the band gap (E_g) [18].

Fig. 2(a) presents the decreasing tendency of the glass transition temperature T_g with the $CdCl_2$ content. The inset in Fig. 2(a) indicates how T_g is determined from the DSC curve. The value of T_g can be evaluated by the Gibbs and DiMarzio model as [19,20]:

$$T_g = \frac{T_0}{[1 - \beta(\langle r \rangle - 2)]} \quad (2)$$

where T_0, β, $\langle r \rangle$ are respectively the transition temperature of the chain akin to the polymer completely (for instance, the S-S chain), the system-dependent constant, and the mean coordination number (MCN) of the network. Eq. (1) indicates the increasing T_g with $\langle r \rangle$, which has been validated by numerous studies of ChGs [21,22]. The average coordination number of Cd in $CdCl_2$ is 4.3 [23], while the coordination numbers of Ge, Sb, S and Cl in glass are 4, 3, 2, 1 according to the (8-N) rule [24]. When GeSbS is replaced by $CdCl_2$, $\langle r \rangle$ is in decline from 2.54 to 2.28, thus T_g decreases. In addition, the increasing density (Fig. 2(b)) is related to the facts that: 1) the average atomic mass of $CdCl_2$ is larger than that of GeSbS, and 2) the atomic packing efficiency (APE) increases as reflected by the descending trend of molar volume [25] (Fig. 2(b)).

With the increasing density, the linear refractive indices (n_0) of the glass samples increases accordingly (Fig. 3). In principle, the transmission of glass decreases as the refractive index increases, which is observed experimentally as illustrated in the transmission spectra (Fig. 1). There is a compromise between the glass transparency and thermal stability. With the replacement of GeSbS by $CdCl_2$, T_g decreases from 280 °C ($x = 0$) to 222 °C ($x = 60$). However, even the sample of the lowest T_g studied in this work has a larger T_g value than that of the well recognized optical switching glass—As_2S_3 (T_g ~185 °C) [15]. It is possible to further improve the thermal stability of the glass by compositional tuning.

The structural modification role of $CdCl_2$ is demonstrated in the

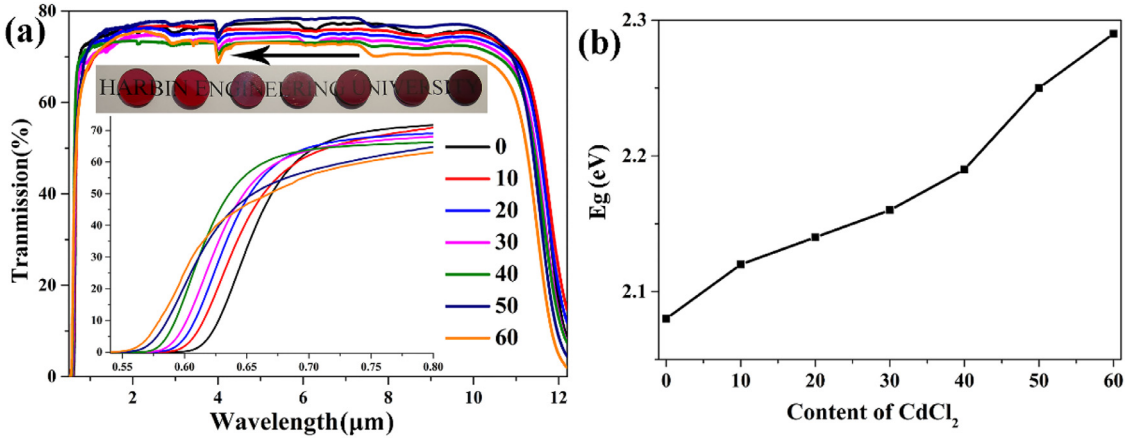

Fig. 1. (a) Transmission spectra and (b) compositional dependence of optical band gaps (E_g) of the samples (100-x) ($60GeS_2$-$40Sb_2S_3$). x $CdCl_2$ (x = 0, 10, 20, 30, 40, 50, 60, in mol.%) with a thickness of 1.0 mm. Insets in (a) are the magnified spectra in the region of short cut-off, and the digital photos of the samples.

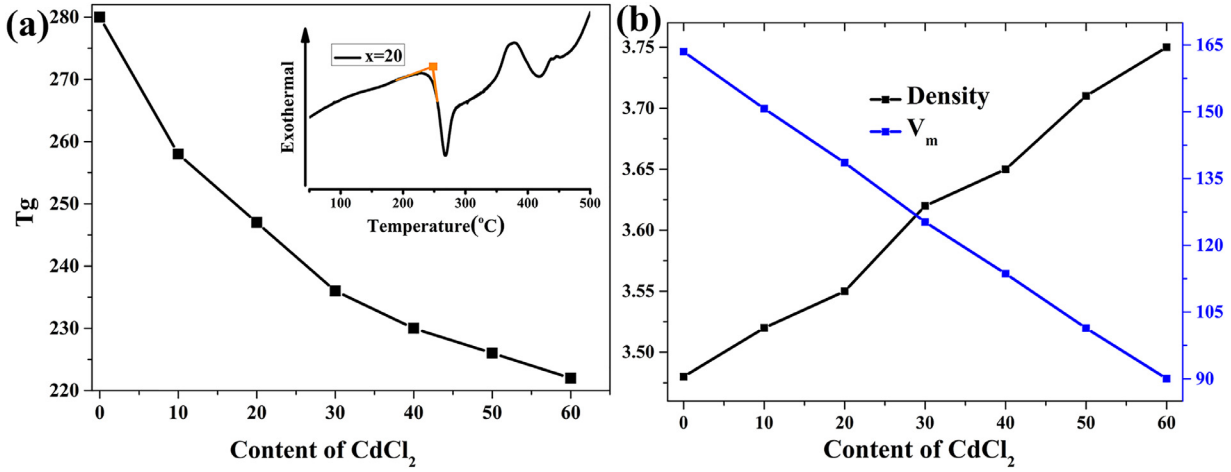

Fig. 2. Variations of (a) glass transition temperature (T_g), (b) density (g/cm^3) and molar volume (Vm, cm^3/mol) as a function of the $CdCl_2$ content (x). The inset in (a) is a representative DSC curve (x = 20) indicating how T_g is determined.

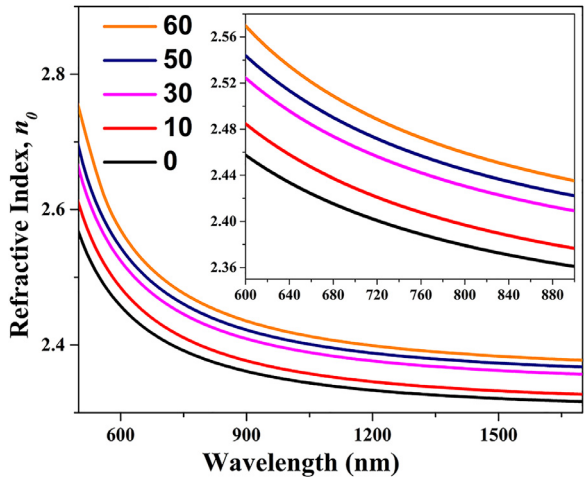

Fig. 3. Refractive indices of the samples (100-x) ($60GeS_2$-$40Sb_2S_3$). x $CdCl_2$ (x = 0, 10, 30, 50, 60, in mol.%). Inset is the magnified part of the spectra.

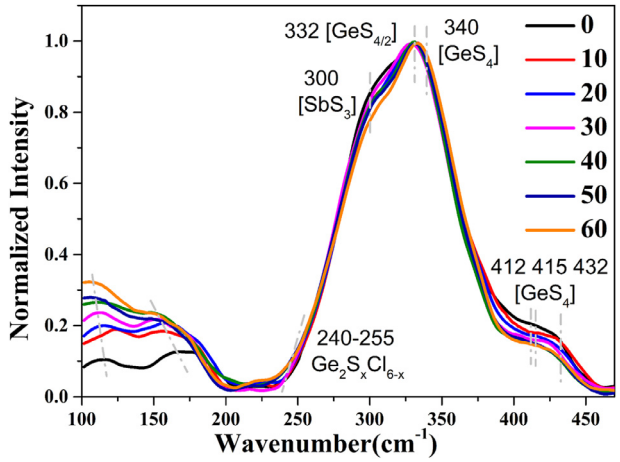

Fig. 4. Normalized Raman spectra of the samples (100-x) ($60GeS_2$-$40Sb_2S_3$). x $CdCl_2$ (x = 0, 10, 20, 30, 40, 50, 60, in mol.%).

normalized Raman spectra as shown in Fig. 4. When GeSbS is substituted by $CdCl_2$, the band intensities decrease at 300 cm^{-1} attributed to the E modes of [$SbS_{3/2}$] unit [26], 332 cm^{-1} to the A_1 modes of corner-sharing [$GeS_{4/2}$] groups [27], and 340 cm^{-1} to the A_1 modes of [GeS_4] tetrahedral unit [28]. Whereas, the bands ranged in 100–200 cm^{-1} arise. The changes might be caused by the partial incorporation of Cl into the [SbS_3] unit, forming the mixed anion [$SbS_xCl_{(3-x)}$] unit. The assignment of the above unit is referred to the formation of the mixed anion [$GaS_{4-x}Cl_x$] unit in the Ga-Sb-S-CsCl system [29] and [SbSI] in GeS_2–SbSI system as explained in our previous work [30]. However, because of the lack of the direct reference, the assignment is still open to discussion. Meanwhile, the 412, 415, 432 cm^{-1} bands belong to [GeS_4] unit weakens, and a new band at 240–255 cm^{-1} increases slightly. The latter band is originated from [$Ge_2S_xCl_{6-x}$] [31] or [GeS_xCl_{4-x}] [32] units. The results above suggest the [GeS_4] unit is transformed into the mixed anion units due to the preferentially formation of the Ge—Cl bond compared with the Ge—S bond with lower affinity. The network breaking role played by $CdCl_2$ may also partly explain the decline in T_g.

The TONL properties of the samples were studied using the Z-scan method. Take the x = 10 glass for example, its closed-aperture (CA) and open-aperture (OA) traces are shown in Fig. 5. The peak-following-valley trace in Fig. 5(a) indicates the positive value of n_2, while the valley trace shown in Fig. 5(b) indicates the reverse-saturated absorption. Because the normalized photon energy ($h\nu/E_g$) of the samples (shown in Table 1) falls between 0.6 and 0.8, within the two-photon absorption (TPA) range ($0.5 < h\nu/E_g < 1$) [33,34], the TONL properties of the glasses is the TPA process. Thus, the TPA coefficient (β_{TPA}) can be evaluated by fitting the CA and OA traces according to the TPA model. The normalized CA and OA results are fitted by the Gaussian decomposition (GD) method [35,36]:

$$T = 1 + \frac{4X}{(X^2+9)(X^2+1)}\Delta\Phi_0 \quad (3)$$

$$T = 1 - \frac{1}{\sqrt{2}(X^2+1)}\Delta\Psi_0 \quad (4)$$

where X is the relative distance between the sample and the focal plane, and $X = z/z_0 = 2z/k\omega_0^2$, among which, z, z_0, k and ω_0 are respectively the actual distance between the sample and the focal plane, the Rayleigh range of the light, the wavenumber of the light and the beam waist at the focal plane.

The differences of transmittance ΔT_v and ΔT_{p-v} can be obtained from the fitting curves in CA and OA traces, then the n_2 and β_{TPA} can be calculated by the following equations [40]:

$$\Delta T_{p-v} = 0.406(1-S)^{0.25}|\Delta\Phi_0| = 0.406(1-S)^{0.25}\frac{2}{\lambda}n_2 I_0 L_{eff} \quad (5)$$

$$\Delta T_v = \Delta\Psi_0 = \beta I_0 L_{eff}/2 \quad (6)$$

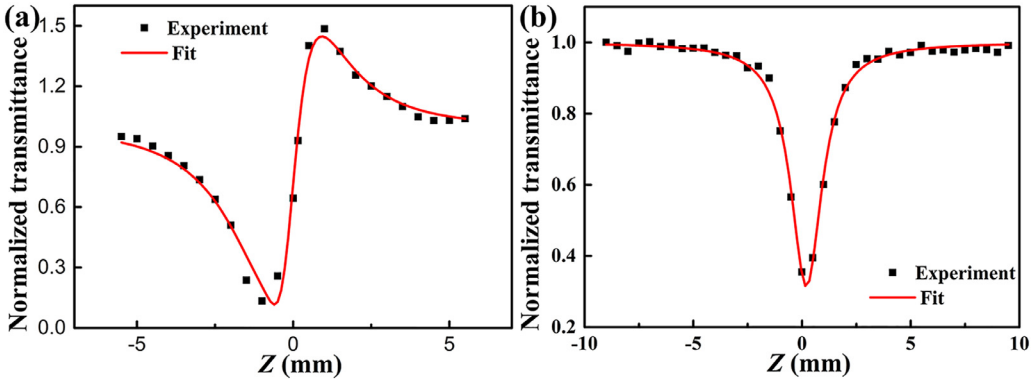

Fig. 5. (a) Closed-aperture (CA), and (b) open-aperture (OA) Z-scan traces of a representative sample (x = 10). The solid lines are theoretical fitting curves.

Table 1
Linear and nonlinear optical parameters of the glasses and some selected glasses for reference.

Composition	n_0	Normalized phononenergy ($h\upsilon/E_g$)	$n^2(10^{-13}$ cm^2/W)	β_{TPA}(cm/GW)	FOM
x = 0	2.58	0.75	9.26	9.68	1.67
x = 20	2.51	0.72	8.28	7.01	1.36
x = 40	2.46	0.71	7.20	5.32	1.18
X = 60	2.42	0.68	6.14	2.40	0.62
SiO_2	1.5	–	0.003	<0.01	<10
As_2S_3	–	–	0.25	2	16.96
60GeS_2-25Sb_2S_3-15CdS	2.4	0.72	0.32	1.08	5.40

SiO_2: measured by the third harmonic generation method at 1550 nm [37].
As_2S_3: measured by the Z-scan method at 1064 nm [38].
60GeSe-25Sb_2S_3-15CdS glass: measured by the Z-scan method at 800 nm [39].
Errors of n_2 and β are approximately 20%, which is within the acceptable limits [9].

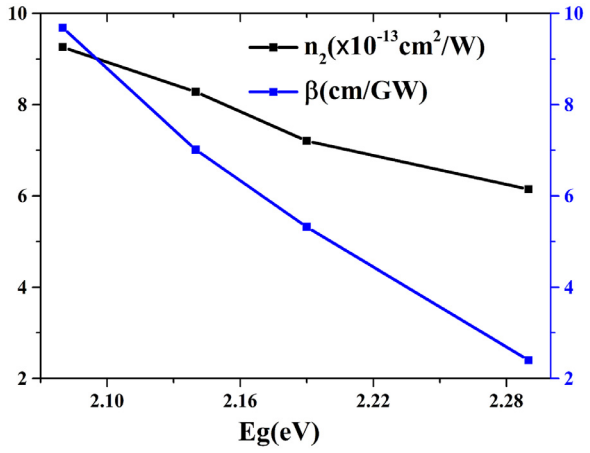

Fig. 6. Evolutions of n_2 and β as a function of the glasses' band gap (E_g).

where S is transmittance of the flare stop, I_0 is the power density of the laser, λ is the wavelength of laser, *Leff* is the effective thickness of the sample. Errors of n_2 and β are approximately 20%, which is within the acceptable limits [9].

The figure of merit (FOM) can be evaluated by FOM = $2\beta_{TPA}\lambda/n_2$. The obtained parameters are also listed in Table 1, and compared with some reference glasses (e.g., silica, As_2S_3 etc.). With the replacement of GeSbS by $CdCl_2$, n_2 and β_{TPA} decrease at different rates (as shown in Fig. 6). In fact, because β_{TPA} decreases more rapidly, the requirement of FOM <1 to meet the optical switching criterion [41] can be achieved for the sample with x = 60. One would expect an even lower value of FOM for higher $CdCl_2$ concentrations, however, the glass becomes hygroscopic then. Seen from Table I, the n_2 of the glass is thousand times greater than that of silica glass, and twenty times of the well-established As_2S_3 and 60GeS_2-25Sb_2S_3-15CdS glasses. The evolution of n_2 with E_g seems close to the E_g^{-4} dependence derived by Sheik-Bahae et al. [42], which means that n_2 will strongly influenced by E_g. With such a high nonlinear refractive index and satisfactory FOM, the newly developed glasses would be a promising photonic material for all optical switching.

4. Conclusion

The addition of $CdCl_2$ extends the visible-light transparency range by ~50 nm as a result of the enlarged optical bandgap. The glass transition temperature decreases with the decrease in the mean coordination number of the network. A compromise has to be considered between extending the glass transparency and maintaining simultaneously the thermal stability. The third-order optical nonlinearity can be well accounted for by the TPA process. Both the nonlinear refractive index and the two-photon absorption coefficient reduce with the content of $CdCl_2$ and are inversely proportional to the bandgap, in conformity with the Sheik-Bahae's rule. Because the two-photon absorption coefficient deceases faster than the nonlinear refractive index does, a good figure of merit (FOM < 1) for all-optical switching can be achieved.

Declaration of Competing Interest

There are no conflicts of interest.

Acknowledgement

This work was financial supported by National Key R&D Program of China(2016YFE0126500), National Natural Science Foundation of China (51872055, 61575050, and 61475189), the Fundamental Research Funds for the Central Universities (HEUCFG201841), the Open Fund of the State Key Laboratory on Integrated Optoelectronics (IOSKL2016KF03), Natural Science Foundation of Heilongjiang Province of China (F2017006), and the 111 project (B13015) to the Harbin Engineering University, Romanian Ministry of Research and Innovation in the Framework of Core Program PN19-03 (21 N/08.02.2019) and Romania-China Bilateral Project PN-III-P3-3.1-PM-RO-CN-2018-0076.

References

[1] B.J. Eggleton, B. Luther-Davies, K. Richardson, Chalcogenide photonics, Nat.

Photon. 5 (2011) 141.
[2] L. Li, H. Lin, S. Qiao, Y. Zou, S. Danto, K. Richardson, J.D. Musgraves, N. Lu, J. Hu, Integrated flexible chalcogenide glass photonic devices, Nat. Photon. 8 (2014) 643.
[3] K. Ogusu, J. Yamasaki, S. Maeda, M. Kitao, M. Minakata, Linear and nonlinear optical properties of Ag–As–Se chalcogenide glasses for all-optical switching, Opt. Lett. 29 (2004) 265–267.
[4] M. Asobe, T. Ohara, I. Yokohama, T. Kaino, Low power all-optical switching in a nonlinear optical loop mirror using chalcogenide glass fibre, Electron. Letts. 32 (1996) 1396–1397.
[5] Z. Han, P. Lin, V. Singh, L. Kimerling, J. Hu, K. Richardson, A. Agarwal, D.T.H. Tan, On-chip mid-infrared gas detection using chalcogenide glass waveguide. Appl. Phys. Lett. 108 (2016) 141106.
[6] J.W. Choi, Z. Han, B.-.U. Sohn, G.F.R. Chen, L.C. Kimerling, K.A. Richardson, A.M. Agarwal, D.T.H. Tan, In supercontinuum generation beyond 2 μm in GeSbS waveguides, Frontiers in Optics, Optical Society of America, Rochester, New York, 2016.
[7] J.W. Choi, Z. Han, B.-.U. Sohn, G.F.R. Chen, C. Smith, L.C. Kimerling, K.A. Richardson, A.M. Agarwal, D.T.H. Tan, Nonlinear characterization of GeSbS chalcogenide glass waveguides, Sci. Rep. 6 (2016) 39234.
[8] L. Ying, C. Lin, Y. Xu, Q. Nie, F. Chen, S. Dai, Glass formation and properties of novel GeS_2–Sb_2S_3–In_2S_3 chalcogenide glasses, Opt. Mater. (Amst) 33 (2011) 1775–1780.
[9] R. Jing, L. Bo, T. Wagner, H. Zeng, G. Chen, Third-order optical nonlinearities of silver doped and/or silver-halide modified Ge–Ga–S glasses, Opt. Mater. 36 (2014) 911–915.
[10] Z. Zhao, A novel chalcohalide fiber with high nonlinearity and low material zero-dispersion via extrusion, J. Am. Ceram. Soc. 102 (2019) 5172–5179.
[11] Z. Zhao, B. Wu, X. Wang, Z. Pan, Z. Liu, P. Zhang, X. Shen, Q. Nie, S. Dai, R. Wang, Mid-infrared supercontinuum covering 2.0–16 μm in a low-loss telluride single-mode fiber, Laser Photon. Rev. 11 (2017) 1700005.
[12] J. Qiu, A. Yang, M. Zhang, L. Li, B. Zhang, D. Tang, Z. Yang, Ga_2S_3-Sb_2S_3-CsI chalcohalide glasses for mid-infrared applications, J. Am. Ceram. Soc. 100 (2017) 5107–5112.
[13] R. Jing, Y. Guang, Z. Huidan, C. Guorong, K. Tanaka, K. Fujita, S. Murai, Y. Tsujiie, Second-Harmonic generation in thermally poled chalcohalide glass, Opt. Lett. 31 (2006) 3492–3494.
[14] Y. Yang, T. Sun, C. Lin, S. Dai, X. Zhang, W. Ji, F. Chen, Performance modification of third-order optical nonlinearity of chalcogenide glasses by nanocrystallization, Ceram. Int. (2019).
[15] A. Feltz, Amorphous Inorganic Materials and Glasses, VCH, 1993.
[16] Z. Yang, L. Luo, W. Chen, Red color $GeSe_2$-based chalcohalide glasses for infrared optics, J. Am. Ceram. Soc. 89 (2006) 2327–2329.
[17] J.E. Huheey, E.A. Keiter, R.L. Keiter, O.K. Medhi, Inorganic Chemistry: Principles of Structure and Reactivity, Pearson Education India, 2006.
[18] L. Calvez, H.L. Ma, J. Lucas, X.H. Zhang, Selenium-Based glasses and glass ceramics transmitting light from the visible to the Far-Ir, Adv. Mater. 19 (2007) 129–132.
[19] X. Lu, Z. Lai, R. Zhang, H. Guo, J. Ren, L. Strizik, T. Wagner, G. Farrell, P. Wang, Ultrabroadband mid-infrared emission from Cr^{2+}-Doped infrared transparent chalcogenide glass ceramics embedded with thermally grown Zns nanorods, J. Euro. Ceram. Soc. 39 (2019) 3373–3379.
[20] A. Sreeram, D. Swiler, A. Varshneya, Gibbs-dimarzio equation to describe the glass transition temperature trends in multicomponent chalcogenide glasses, J. Non-Crystal. Solids. 127 (1991) 287–297.
[21] Y. Yang, B. Zhang, A. Yang, Z. Yang, P. Lucas, Structural origin of fragility in Ge–As–S glasses investigated by calorimetry and Raman spectroscopy, J. Phys. Chem. B 119 (2015) 5096–5101.
[22] R.P. Wang, A. Smith, A. Prasad, D.Y. Choi, B. Luther-Davies, Raman spectra of $Ge_xAs_ySe_{1-x-y}$ glasses, J. Appl. Phys. 106 (2009) 043520.
[23] O. Babushkina, S. Volkov, Raman spectroscopy of the heteronuclear complexes in the $ZnCl_2$, $CdCl_2$- Li, K/Cl and $AlCl_3$, $MgCl_2$- Li, K/Cl melts, J. Mol. Liquids 83 (1999) 131–140.
[24] R. Jing, Y. Guang, Z. Huidan, Z. Xianghua, Y. Yunxia, C. Guorong, Properties of Dy^{3+}-Doped Ge–As–Ga–Se chalcogenide glasses, J. Am. Ceram. Soc. 89 (2006) 2486–2491.
[25] X. Lu, Y. Zhang, J. Ren, E. Lewis, G. Farrell, A. Yang, Z. Yang, P. Wang, Chalcogenide glasses with embedded ZnS nanocrystals: potential mid-infrared laser host for divalent transition metal ions, J. Am. Ceram. Soc. 101 (2018) 666–673.
[26] L. Petit, N. Carlie, K. Richardson, Y. Guo, A. Schulte, B. Campbell, B. Ferreira, S. Martin, Effect of the substitution of S for Se on the structure of the glasses in the system $Ge_{0.23}Sb_{0.07}S_{0.70}-xSe_x$, J. Phys. Chemi. Solids 66 (2005) 1788–1794.
[27] Q. Mei, J. Saienga, J. Schrooten, B. Meyer, S.W. Martin, Preparation and characterization of glasses in the $Ag_2S+B_2S_3+GeS_2$ system, J. Non Cryst. Solids. 324 (2003) 264–276.
[28] C. Julien, S. Barnier, M. Massot, N. Chbani, X. Cai, A.M. Loireau-Lozac'h, M. Guittard, Raman and infrared spectroscopic studies of Ge-Ga-Ag sulphide glasses, Mater. Sci. Eng. B. 22 (1994) 191–200.
[29] M. Zhang, Z. Yang, H. Zhao, A. Yang, L. Li, H. Tao, Glass form ing and properties of Ga_2S_3-Sb_2S_3-CsCl chalcohalide system, J. Alloy. Compd. 722 (2017) 166–172.
[30] L. Ding, R. Jing, H. Jain, D. Zhao, G. Yang, G. Chen, Self-reversible Photodarkening of the mixed Ges_2–SbSi glasses, J. Am. Ceram. Soc. 94 (2011) 1657–1660.
[31] C. Lin, L. Calvez, Z. Li, S. Dai, H. Tao, H. Ma, X. Zhang, B. Moine, X. Zhao, Enhanced up-conversion luminescence in Er^{3+}-Doped 25GeS_2-35Ga_2S_3-40CsCl chalcogenide glass–ceramics, J. Am. Ceram. Soc. 96 (2013) 816–819.
[32] T. Haizheng, Z. Xiujian, J. Chengbin, Y. Hui, M. Shun, Raman scattering studies of the GeS_2–Ga_2S_3–CsCl glassy system, Solid State Commun. 133 (2005) 327–332.
[33] F. Théberge, P. Mathieu, N. Thiré, J.-.F. Daigle, B.E. Schmidt, J. Fortin, R. Vallée, Y. Messaddeq, F. Légaré, Mid-Infrared nonlinear absorption in As_2S_3 chalcogenide glass, Opt. Express 24 (2016) 24600–24610.
[34] K. Tanaka, Two-photon optical absorption in amorphous materials, J. Non-Crystal. Solids 338 (2004) 534–538.
[35] M. Yin, H.P. Li, S.H. Tang, W. Ji, Determination of nonlinear absorption and refraction by single Z-Scan method, Appl. Phys. B 70 (2000) 587–591.
[36] B. Gu, K. Lou, J. Chen, H.-.T. Wang, W. Ji, Determination of the nonlinear refractive index in multiphoton absorbers by Z-Scan measurements, J. Opt. Soc. Am. B 27 (2010) 2438–2442.
[37] D. Milam, Review and assessment of measured values of the nonlinear refractive-index coefficient of fused silica, Appl. Opt. 37 (1998) 546–550.
[38] F. Smektala, C. Quemard, L. Leneindre, J. Lucas, A. Barthélémy, C. De Angelis, Chalcogenide glasses with large non-linear refractive indices, J. Non-Crystal. Solids 239 (1998) 139–142.
[39] H. Guo, C. Hou, F. Gao, A. Lin, P. Wang, Z. Zhou, M. Lu, W. Wei, B. Peng, Third-Order nonlinear optical properties of GeS_2-Sb_2S_3-CdS chalcogenide glasses, Opt. Express 18 (2010) 23275–23284.
[40] M. Sheik-Bahae, A.A. Said, T. Wei, D.J. Hagan, E.W.V. Stryland, Sensitive measurement of optical nonlinearities using a single beam, IEEE J. Quantum Electron. 26 (1990) 760–769.
[41] V. Mizrahi, K.W. DeLong, G.I. Stegeman, M.A. Saifi, M.J. Andrejco, Two-photon absorption as a limitation to all-optical switching, Opt. Lett. 14 (1989) 1140–1142.
[42] M. Sheik-Bahae, D.J. Hagan, E.W. Van Stryland, Dispersion and band-gap scaling of the electronic kerr effect in solids associated with two-photon absorption, Phys. Rev. Letts. 65 (1990) 96–99.